Model for the Interactions between Anionic Dendrimers and Cationic Surfactants by Means of the Spin Probe Method

M. Francesca Ottaviani,*,† Pablo Andechaga,† Nicholas J. Turro,‡ and Donald A. Tomalia§

Department of Chemistry, University of Florence, 50121 Florence, Italy, Department of Chemistry, Columbia University, New York, New York 10027, and Michigan Molecular Institute, Midland, Michigan 48640

Received: October 22, 1996; In Final Form: May 13, 1997[⊗]

The supramolecular structures formed when anionic polyamidoamine starburst dendrimers, in the presence of low concentrations of spin probe surfactants, are added to aqueous solutions of nonlabeled cationic surfactants have been investigated by EPR spectroscopy. In order to obtain an overview of dendrimer/surfactant systems, a variety of spin probe surfactants, differing from one another in chain length, structure, polarity, charge, solubility, and self-aggregating ability, were employed. Computer simulation of the experimental EPR spectra allowed evaluation of mobility and polarity parameters of the spin probes in the supramolecular structures formed in addition to determination of the degree of partitioning of the probe among various supramolecular structures. Depending on the concentrations of both the surfactant and the dendrimer, the dendrimer size, and temperature, the model envisions two types of structures, i.e., primary structures consisting of probe monomers adsorbed on the dendrimer surface and secondary structures consisting of probe monomers adsorbed in surfactant aggregates bound to the dendrimer surface. Depending on the probe concentration and on the probe solubility into the surfactant aggregates, line broadening was observed, which was consistent with spin−spin interactions supporting a model in which more than one probe was inserted in the aggregates. This solubility was enhanced by the presence of dendrimers and by increasing temperature.

Introduction

Electron paramagnetic resonance (EPR) spectroscopy has provided a powerful tool for the investigation of the aggregation behavior of surfactants in aqueous solution, in particular through the use of probes that are surfactants possessing a spin label and capable of inserting into micellar structures.[1−10] Micelles serve an important scientific role as primitive structures to mimic biological structures and an important practical role for a range of biological and industrial processes. The interactions of surfactants and micelles with macromolecules and polyelectrolytes are of particular interest, since these systems include those originated by surfactants interacting with biological macromolecules, such as proteins and DNA.[11−15]

Recently, we have applied the EPR spin probe technique to investigate the supramolecular structures formed when surfactants are added to aqueous solutions of dendritic polymers.[9,10] Dendrimers are supramolecular structures possessing nanoscopic sizes and well-defined composition and constitution, characterized by branched repeating units (layers termed generations, *G*) emanating from a central core.[16,17] We have investigated the supramolecular structures formed by interactions of surfactants with the polyamidoamine family of starburst dendrimers (SBDs) possessing branches consisting of amidoamine units covalently linked in layers emanating from a central amino core.[18] The branches at the external surface may terminate with amino groups (full generations, $G = n.0$) or carboxylate groups (half generations, $G = n.5$) with sodium gegenions, as an example. Previous EPR investigations[19,20] have shown that the external and internal structures and interacting ability are similar to those of biomacromolecules such as proteins and enzymes.

Molecular simulations[21] of the SBD structure have shown that a change in the dendrimer morphology occurs for the $n.0$ *G* systems at around $G = 4.0$. Thus, the SBD may be classified as "earlier" (*G* less than 4) or "later" generations (*G* greater than 4), with $G = 4$ being a borderline case. The earlier generations are characterized by an open and solvent accessible external structure, whereas the later generations are characterized by a densely packed external surface. Chart 1 schematically shows, as an example, the SBD structure for $G = 3.5$. In the present study, $G = 3.5$ and $G = 7.5$ were selected as representative of the earlier and later generations.

We are concerned with the structures and dynamics resulting from interactions of the anionic SBDs with surfactants and micellar aggregates and the aggregational processes of surfactants in the presence of anionic dendrimers. We have selected cationic surfactants in order to promote the electrostatic interactions between the surface of the dendrimers and the charged head groups of the surfactants. Two thoroughly investigated surfactants, trimethylammonium dodecyl bromide (DTAB) and trimethylammonium hexadecyl bromide (CTAB), were chosen for detailed investigation. Their formulas are reported in Chart 1. The EPR spin probe method was selected as the technique for investigation of the interactions of surfactants with SBDs because of its demonstrated ability to provide information on the structure and dynamics of the supramolecular structures formed in systems involving micellar and related aggregates.

A multiple probe technique was employed in this investigation to provide information concerning the structure and dynamics of cationic surfactant−anionic polyelectrolyte systems. Preliminary EPR measurements were conducted in the absence and in the presence of the dendrimers in order to identify the probes to best monitor, through spectroscopic parameters, the dynamics, the environmental polarity, and the partition coefficients resulting from interactions of surfactants, surfactant micelles, and dendrimers.

The formulas of the probes finally chosen for the present study, that is, C12T, CAT9, and CAT16, are reported in Chart 1.

* To whom correspondence should be addressed.
† University of Florence.
‡ Columbia University.
§ Michigan Molecular Institute.
⊗ Abstract published in *Advance ACS Abstracts,* July 1, 1997.

S1089-5647(96)03271-3 CCC: $14.00

CHART 1

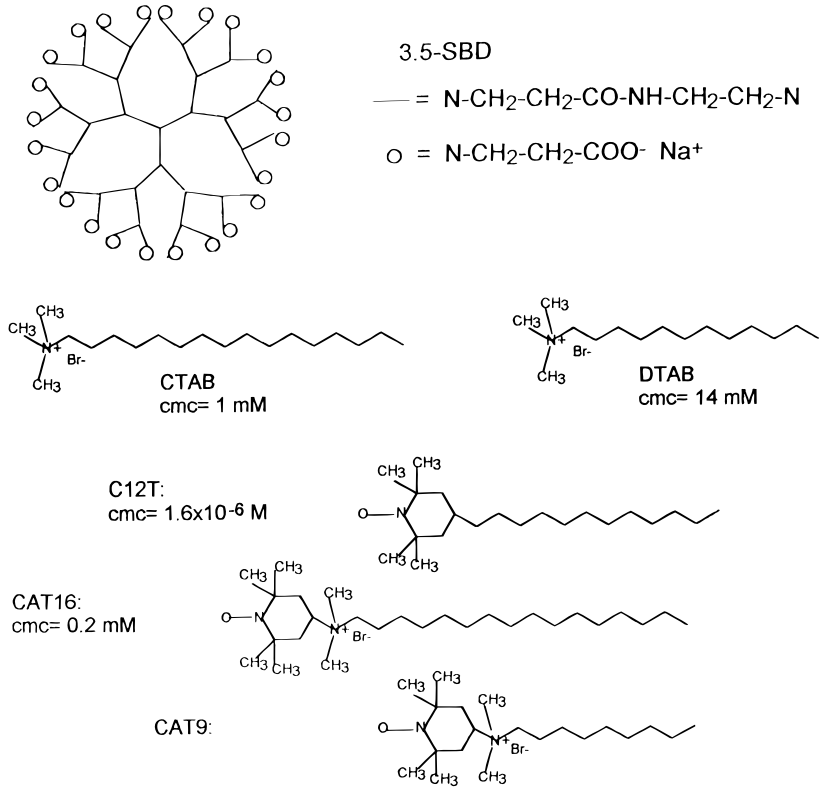

In a previous investigation[22] the CAT*n* probes were shown to interact with the SBD surface both at the hydrophilic head groups of the surfactant and with more hydrophobic sites close to the SBD surface. Previous investigations[9,10] have also probed the aggregation behavior of CAT16 and the formation of mixed CAT16−CTAB micelles. In the latter investigations the EPR line shapes were dominated by the spin−spin interactions due to the aggregation of the probe radical in the micellar structures. Because the presence of spin−spin interactions interferes with measurement of the EPR parameters (mobility, polarity, anisotropy of motion), which provide most of the information on the supramolecular structures and dynamics, in this report the radical surfactants served mainly as probes of environmental properties, for which spin−spin interactions are minimized.

Experimental Section

The water solutions were prepared in doubly distilled water filtered through Millipore filters.

The SBDs employed in this study have been synthesized as described in previous papers.[18] Methyl-ester-terminated generations were hydrolyzed with stoichiometric amounts of NaOH in methanol to obtain carboxylate external groups with sodium gegenions. Accurate purification of the dendrimers was accomplished from subsequent recrystallization in water solutions. The purity was carefully controlled by mass spectrometry.[23] Aqueous solutions of 3.5SBD and 7.5SBD at 0.37 M concentration in surface SBD−COO^- groups were prepared and stored immediately after preparation under nitrogen at about 278 K. The final dendrimer solutions containing the radicals, both in the absence and in the presence of micelles, are at concentrations of 0.031 and 0.185 M in surface carboxylate groups. These two concentrations were selected on the basis of the previous results obtained with the *n*.5SBDs in the presence of CAT16 micelles.[9] These results indicate that low concentrated solutions (represented by [SBD−COO^-] = 0.031 M) show a larger fraction of aggregates at the SBD/water interface with respect to solutions at high concentration (represented by [SBD−COO] = 0.185 M).

Titration as a function of [SBD−COO^-] showed a progressive modification from the EPR data evaluated at [SBD−COO^-] = 0.031 M to the results obtained at [SBD−COO^-] = 0.185 M, and it was not henceforth discussed.

The radical surfactants—C12T, CAT9, CAT16—were purchased from Molecular Probes and used as received. Water solutions of the cationic radicals were prepared at concentration of 2×10^{-4} M. In a series of measurements the radical solution was at the same concentration as the samples in the presence of CTAB or DTAB and/or the dendrimers.

DTAB and CTAB (Sigma) were recrystallized from methanol. Different values for the cmc of CTAB are reported in the literature ranging from 0.75 to 1 mM. We used as reference the cmc evaluated by Berr[24] by means of surface tension, that is cmc(CTAB) = 1 mM. For DTAB we referred to the same cmc (14 mM) as used by Caminati and co-workers in a study on the aggregational behavior of DTAB in the presence of *n*.5SBDs.[25] The starting solutions of the surfactants were prepared well above their cmc, that is, [CTAB] = 8 mM and [DTAB] = 80 mM. These concentrated solutions were warmed at 313 K to provide clear solutions. Conversely, the diluted solutions used in this work were clear at 303 K. Therefore, the EPR spectra, unless otherwise specified, were recorded at 303 K. It was not convenient to record EPR spectra at higher temperature, since the faster exchange of the radicals in different environments often provided a lack of information about the structure and the mobility of each environment.

Titration has been performed as a function of [CTAB] to follow the micellization process of the surfactant−probe system in the absence and in the presence of the dendrimers. Only representative EPR spectra at selected CTAB concentrations are shown and discussed in the Results and Discussion section.

The EPR spectra were recorded by means of a Bruker 200D spectrometer operating in the X band (9.5 GHz), interfaced with

Stelar software to a PC-IBM computer for data acquisition and handling. The temperature was controlled with the aid of a Bruker ST 100/700 variable-temperature assembly. Magnetic parameters were measured by field calibration with the diphenylpycrylhydrazide (DPPH) radical ($g = 2.0036$). An EPR tube (1 mm diameter) containing a few milligrams of solid DPPH was inserted in the EPR cavity together with the samples to be examined.

Results and Discussion

The results obtained from each probe under various experimental conditions are discussed separately and then compared in order to devise a general model to describe the structure and dynamics of the cationic surfactant−anionic dendrimer systems.

Computation of the Spectra and Main Derived EPR Parameters. Quantitative information on the mobility, the environmental polarity, and partition coefficients was extracted from the observed EPR spectra through computer-assisted analysis of the line shape employing the broadly accepted procedure of Schneider and Freed.[26] Three sets of magnetic parameters (the components of the **g** tensor, for the Zeeman coupling between the electron spin and the magnetic field, and the components of the $\mathbf{A_N}$ tensor, for the hyperfine coupling between the electron spin and the nuclear spin) were used for the computation of the spectra in this study. These sets of parameters were indicated, for simplicity, as "f" and "m". The letter "f" refers to "free" radicals which are in the bulk aqueous phase or interacting as monomers with the dendrimer surface (primary interactions).[22,25] The letter "m" refers to radicals in micellar aggregates whose structures are under investigation. The insertion of the radical probe into a micellar structure places the nitroxide group into a partially hydrophobic medium.[6] In turn, this leads to a decrease of the $\mathbf{A_N}$ components, corresponding to a decrease in $\langle A_N \rangle = (A_{XX} + A_{YY} + A_{ZZ})/3$, which reflects the lower polarity of the environment sensed by the radical.[27] The parameters indicated as f and m were obtained by computing the spectra at 298 and 77 K of CAT9 solutions in the absence and in the presence of DTAC micelles, respectively. These parameters held for CAT9 and C12T samples in the absence and in the presence of micelles, also upon addition of the dendrimers, and for CAT16 samples in the absence of the dendrimers. The computation of the spectra of CAT16−CTAB aggregates in the presence of the dendrimers indicated a lower polarity of the radical environment, when inserted in the micelles, which corresponded to the introduction of the set of parameters henceforth indicated as m′. The sets of magnetic parameters used in the computation are as follows (accuracy ca. 1×10^{-4} for g_{ii} and ca 0.1 G for A_{ii}, the accuracy was estimated on the basis of the spectral modifications which led to significant lack of fitting between computed and experimental line shape):

m: $g_{xx}, g_{yy}, g_{zz} = 2.0090, 2.0064, 2.0039$;
$A_{xx}, A_{yy}, A_{zz} = 6.5$ G, 7.5 G, 34.7 G

m′: $g_{xx}, g_{yy}, g_{zz} = 2.0092, 2.0064, 2.0040$;
$A_{xx}, A_{yy}, A_{zz} = 6.0$ G, 6.5 G, 33.7 G

f: $g_{xx}, g_{yy}, g_{zz} = 2.0088, 2.0062, 2.0035$;
$A_{xx}, A_{yy}, A_{zz} = 6.8$ *G*, 8.2 *G*, 35.7 G

A Brownian rotation diffusion is assumed to modulate the magnetic parameters. The approximate cylindrical symmetry of the radicals allows the assumption that there are two main components of the rotational correlation time, i.e., $\tau_\perp$ and $\tau_\parallel$. $\tau_\perp$ is the most relevant dynamical parameter in the case where the main rotational axis lies in the direction of the p_z orbital containing the unpaired electron.

The accuracy in the evaluation of the correlation time for motion is estimated to be 5%.

When more than one radical probe occupies a single micellar aggregate, collisions of the radicals within the constraint of the aggregate result in significant Heisenberg spin exchange.[28] These authors assume a proportionality between the spin−spin exchange frequency, ω_{ex}, and the local concentration of the radicals. Therefore, ω_{ex} is considered as an indicator of the formation of radical aggregates, and the variation in ω_{ex} as a measure of variation of the local concentration of the probes. Aggregates containing different numbers of probes should contribute to the overall line shape. However, we consider, for simplicity, a homogeneous distribution of the radicals in the aggregates and the calculated ω_{ex} may be considered as an averaged value (accuracy in the evaluation = 5%).

In some situations radicals are distributed in two or more environments and undergo a slow exchange on the EPR time scale. Such situations require the addition of two or more spectral components to simulate the observed EPR line shape. Evaluation of the different percentages of the individual components (estimated accuracy = 2%) allowed an estimation of the relative probe quantity in each environment. Attempts to simulate more than three components is problematical both mathematically (too many parameters and reduction of accuracy) and in terms of physical interpretation (ambiguity of structural assignments). As a result, the analyses performed were limited to a maximum of three components and where possible within the desired precision of simulation were limited to two components.

The variation of each parameter produced a different modification of the computed line shape and the goodness of the fitting was assessed by varying each parameter, which also verified the accuracy in the calculation. In the case of two or three spectra constituting the overall EPR signal, the reliability of the calculated parameters was ensured by means of a subtraction−addition procedure of spectra obtained in different experimental conditions. This procedure provided the single components of the spectra, which were computed and then added at the proper relative amounts to reproduce the experimental line shape.

C12T as a Probe of CTAB Micellization in the Absence and in the Presence of Dendrimers. Figure 1 shows the experimental EPR (full lines) and computed (dotted lines) spectra for aqueous solutions of C12T (2×10^{-5} M) with CTAB ($< 2 \times 10^{-3}$ M) in the absence of dendrimers (a); CTAB (5×10^{-4} M) + 3.5 SBD (0.031 M) (b); or + 7.5 SBD (0.031 M (c) and 0.185 M (d)). The parameters obtained from computation of the spectra are reported in Table 1-Figure 1.

C12T presents a very low cmc, that is, 1.6×10^{-6} M.[6] The titration as a function of [CTAB] showed that, for [CTAB] < 2×10^{-3} M, the spectrum corresponds mainly (95%) to C12T radicals forming micelles in equilibrium with a small portion (5%) of radicals in the aqueous phase. It is expected that above the reported cmc for CTAB (1×10^{-3} M), mixed micelles of CTAB and C12T would be formed and that this would be reflected in the line shape of the EPR as the spin−spin interactions were varied. However, from the Heisenberg exchange frequency, it appears that the progressive dilution of C12T in CTAB micelles only started at CTAB concentrations above 2×10^{-3} M, i.e., well above the cmc. Two possible explanations for this result are (1) the formation of mixed micelles of C12T and CTAB is not favored energetically and

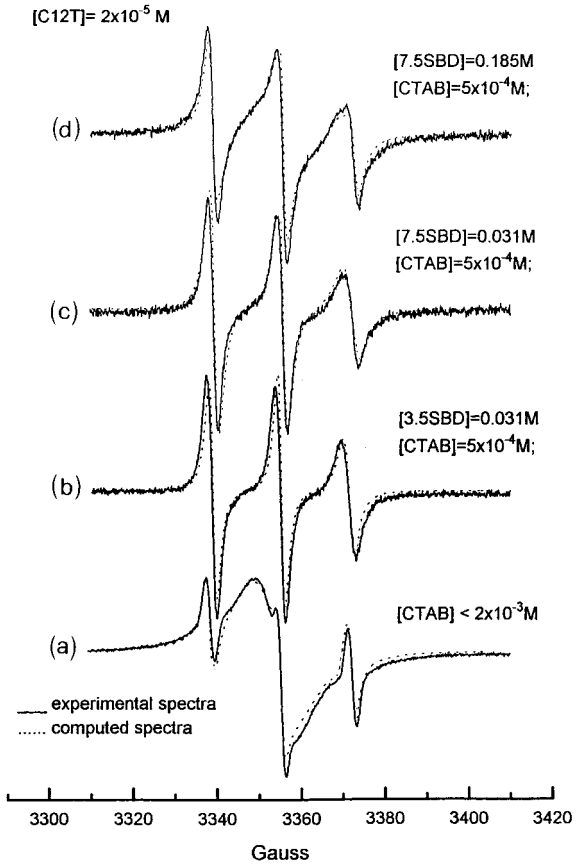

Figure 1. Experimental (full lines, 303 K) and computed (dotted lines) EPR spectra for aqueous solutions of CTAB ($<2 \times 10^3$ M) containing C12T (2×10^{-5} M) in the absence of dendrimers and of CTAB (5×10^{-4} M) in the presence of 3.5 SBD (0.031 M) and 7.5 SBD (0.031 and 0.185 M).

(2) the cmc of CTAB is shifted toward higher concentration in the presence of C12T. The observation (results not shown) that an increase in temperature leads to more efficient insertion of C12T into CTAB micelles favors explanation 1.

The exchange-narrowed component due to C12T radicals in the same aggregate disappeared upon addition of dendrimers to solutions of CTAB (5×10^{-4} M) in the presence of both 3.5 SDB and 7.5 SBD for dendrimer concentrations as low as 0.031 M. The probe environment reported a reduced mobility and low polarity ($\tau_\perp$ and the set m of A_{ii} components, in Table 1-Figure 1) compared to radicals in the aqueous phase, suggesting the insertion of the probe into CTAB aggregates. Since the formation of mixed CTAB−C12T aggregates was promoted by adding the dendrimers and the decrease in mobility of C12T was indicative of the interaction with the dendrimer surface, the CTAB−C12T aggregates were formed at the dendrimer surface. The interaction of the surfactants with the SBD surface was therefore cooperative; that is, aggregates were formed at the SBD/water interface. For the 7.5 SBD samples, the fraction of the probe radicals, which possesses the f set of magnetic parameters, showed a decrease in mobility with respect to the radicals in water solution (from 8×10^{-11} to 3.5×10^{-10} s). Such a decrease has been previously observed[22] in the case of noncooperative primary interactions with the dendrimer surface; that is, the surfactant monomers bind the dendrimer surface by means of both electrostatic and hydrophobic interactions. These previous studies[22] have demonstrated that the surfactant monomers preferentially interact (primary interactions) with the surface of large sized dendrimers (later generations), with respect to smaller dendrimers (earlier generations).

An increase in the concentration of 7.5 SBD to 0.185 M showed the appearance of an exchange-narrowed component, and the parameters reported in Table 1-Figure 1 suggest the following results: (a) more than half of the radicals still retained their micellar structure (the same exchange-narrowed component as observed for C12T micelles is observed); (b) ca. 25% of the C12T radicals form mixed micelles with CTAB; and (c) the remaining fraction of radicals showed primary interactions with the dendrimer surface.

We come to the following conclusions based on computer simulation of the EPR spectra of C12T as a probe: (1) in the absence of dendrimers, the addition of CTAB in concentrations up to 2×10^{-3} M, i.e., above its cmc, does not disrupt the C12T micellar structure; (2) upon addition of the dendrimers to the system formed by separate CTAB and C12T micelles, the signal that we attributed to C12T automicelles disappeared and was replaced with a signal with polarity and mobility suggestive of aggregates of CTAB containing C12T as probes. Since this occurred in the presence of SBDs, we suggest that the aggregates were formed at the dendrimer surface (secondary, cooperative interactions); (3) primary, noncooperative interactions between the radical and the dendrimers were preferred to the insertion of C12T into CTAB micelles formed at the 7.5 SBD surface; (4) an increase in concentration of 7.5 SBD inhibits the formation of dendrimer surface CTAB aggregates containing C12T probes, in spite of the increase of ionic strength, which is known to promote the formation of micellar aggregates at concentrations below the cmc of the surfactants.

CAT16 as a Probe of CTAB Micellization in the Absence and in the Presence of Dendrimers. Figure 2 shows the experimental (full line, 303 K) and the computed (dotted lines) EPR spectra of CTAB solutions (5×10^{-4} M) in the absence (a) and presence of 3.5 SBD (b) and 7.5 SBD (c) (0.031 M); and of CTAB solutions (2×10^{-3} M) in the absence (a′) and presence of 3.5 SBD (b′) and 7.5 SBD (c′) (0.031 M), containing CAT16 at concentrations 100 times lower than the CTAB. The parameters derived from the simulation of the spectra in Figure 2 are reported in Table 1-Figure 2.

CAT16 presents a critical micellar concentration (cmc) of 0.2 mM, as evaluated from surface tension measurements.[9,10] The cmc measured from EPR spectral analysis is higher, that is, about 0.5 mM. Therefore, the concentration of CAT16 in the samples for the spectra in Figure 2 is well below the cmc.

The following conclusions concerning the supramolecular structures formed were obtained from analysis of the spectra in Figure 2. In the absence of SBDs the CTAB aggregates are formed at their cmc as monitored by the CAT16 probe (change in polarity and mobility of the probe at the cmc), and the CAT16 monomers formed mixed micelles with CTAB, but with no more than one probe per micelle (no spin−spin interactions). The fraction of probes inserted in the micelles increased as the CTAB concentration was increased above the cmc.

In the presence of SBDs the signal with the m′ parameters appeared at low CTAB concentration, indicating that CTAB aggregates, different from the ones with the m parameters, were formed at a concentration well below the surfactant cmc. This means that the dendrimers facilitated the formation of aggregates, by offering a surface suitable to a cooperative interaction of the surfactants (aggregates formed at the SBD surface), even with low surfactant concentration. Interestingly, the ω_{ex} included in the calculation indicated that more than one probe was inserted into the CTAB aggregates (in spite of the very low CAT16 concentration with respect to the CTAB concentration). Unexpectedly, the fraction of probes in the CTAB aggregates slightly decreased as the CTAB concentration

TABLE 1: Main Parameters Obtained from the Computation of the EPR Spectra[a]

Figure 1

signal	[C12T]	[CTAB]	*G*	[SBD]	magnetic parameters	%	$\tau_\perp$ (s)	ω_{ex} (s^{-1})
(a)	2×10^{-5}	$<2 \times 10^{-3}$			m	95	(1×10^{-9})	5.5×10^{8}
	2×10^{-5}	$<2 \times 10^{-3}$			f	5	8.0×10^{-11}	
(b)	2×10^{-5}	5×10^{-4}	3.5	0.031	m	100	5.5×10^{-10}	
(c)	2×10^{-5}	5×10^{-4}	7.5	0.031	m	67	5.5×10^{-10}	
	2×10^{-5}	5×10^{-4}	7.5	0.31	f	33	1.0×10^{-10}	
(d)	2×10^{-5}	5×10^{-4}	7.5	0.185	m	53	(1×10^{-9})	5.5×10^{8}
	2×10^{-5}	5×10^{-4}	7.5	0.185	m	25	5.0×10^{-10}	5.0×10^{7}
	2×10^{-5}	5×10^{-4}	7.5	0.185	f	22	3.5×10^{-10}	

Figure 2

signal	[CAT16]	[CTAB]	*G*	[SBD]	magnetic parameters	%	$\tau_\perp$ (s)	ω_{ex} (s^{-1})
(a)	5×10^{-6}	5×10^{-4}			f	100	8.0×10^{-11}	
(a′)	2×10^{-5}	2×10^{-3}			m	75	4.5×10^{-10}	
	2×10^{-5}	2×10^{-3}			f	25	2.0×10^{-10}	
(b)	5×10^{-6}	5×10^{-4}	3.5	0.031	m′	57	5.5×10^{-10}	6.0×10^{7}
	5×10^{-6}	5×10^{-4}	3.5	0.031	f	43	4.0×10^{-10}	
(b′)	2×10^{-5}	2×10^{-3}	3.5	0.031	m′	70	5.5×10^{-10}	6.0×10^{7}
	2×10^{-5}	2×10^{-3}	3.5	0.031	f	30	4.0×10^{-10}	
(c)	5×10^{-6}	5×10^{-4}	7.5	0.031	m′	70	5.5×10^{-10}	6.0×10^{7}
	5×10^{-6}	5×10^{-4}	7.5	0.031	f	30	4.0×10^{-10}	
(c′)	2×10^{-5}	2×10^{-3}	7.5	0.031	m′	55	5.5×10^{-10}	5.0×10^{7}
	2×10^{-5}	2×10^{-3}	7.5	0.031	f	45	4.0×10^{-10}	

Figure 3

signal	[C12T]	[DTAB]	*G*	[SBD]	magnetic parameters	%	$\tau_\perp$ (s)	ω_{ex} (s^{-1})
(c)	2×10^{-5}				m	95	(1×10^{-9})	5.5×10^{8}
	2×10^{-5}				f	5	8.0×10^{-11}	
(a-i)	2×10^{-5}	2.0×10^{-3}			m	50	3.0×10^{-10}	7.0×10^{7}
	2×10^{-5}	2.0×10^{-3}			m	48	(1×10^{-9})	5.0×10^{8}
	2×10^{-5}	2.0×10^{-3}			f	2	8.0×10^{-11}	
(b-i)	2×10^{-5}	7.0×10^{-3}			m	45	(1×10^{-9})	5.0×10^{8}
	2×10^{-5}	7.0×10^{-3}			m	55	6.0×10^{-10}	
(a-ii)	2×10^{-5}	2.0×10^{-3}	7.5	0.185	m	100	3.0×10^{-10}	6.0×10^{7}
(b-ii)	2×10^{-5}	7.0×10^{-3}	7.5	0.185	m	100	4.0×10^{-10}	

Figure 4

signal	[CAT9]	[DTAB]	*G*	[SBD]	magnetic parameters	%	$\tau_\perp$ (s)	ω_{ex} (s^{-1})	*T* (K)
(a)	2×10^{-6}	4.0×10^{-4}			f	100	8.0×10^{-11}		303
(b)	2×10^{-6}	4.0×10^{-4}	3.5	0.031	f	100	2.0×10^{-10}		303
(b)	2×10^{-6}	4.0×10^{-4}	7.5	0.185	f	100	2.0×10^{-10}		303
(c)	2×10^{-6}	4.0×10^{-4}	3.5	0.185	m	65	5.5×10^{-10}		303
	2×10^{-6}	4.0×10^{-4}	3.5	0.185	f	35	2.0×10^{-10}		
(c)	2×10^{-6}	4.0×10^{-4}	7.5	0.031	m	65	5.5×10^{-10}		303
	2×10^{-6}	4.0×10^{-4}	7.5	0.031	f	35	2.0×10^{-10}		
(d)	5×10^{-6}	1.0×10^{-3}	3.5	0.185	m	75	5.5×10^{-10}		303
	5×10^{-6}	1.0×10^{-3}	3.5	0.185	f	25	2.0×10^{-10}		
(e)	5×10^{-5}	1.0×10^{-3}	3.5	0.185	m	95	(1×10^{-9})	1.8×10^{8}	303
	5×10^{-5}	1.0×10^{-3}	3.5	0.185	f	5	5.0×10^{-11}		
(f)	5×10^{-5}	1.0×10^{-3}	7.5	0.185	m	50	(1×10^{-9})	3.5×10^{8}	303
	5×10^{-5}	1.0×10^{-3}	7.5	0.185	f	50	2.0×10^{-10}		
(g)	5×10^{-5}	1.0×10^{-3}	7.5	0.185	m	95	5.5×10^{-10}		333
	5×10^{-5}	1.0×10^{-3}	7.5	0.185	f	5	2.0×10^{-10}		

[a] Accuracy: $\tau_\perp$ and ω_{ex}, 5%. Percentages: 2%.

increased in the presence of 7.5 SBD. It appears that the CAT16 probes reach a "saturation" condition with respect to solubility in CTAB aggregates formed at the 7.5 SBD surface.

In conclusion, the EPR parameters (Table 1-Figure 2) suggest that the structures of the CTAB aggregates are different in the absence and presence of dendrimers. In the presence of dendrimers the environment is less polar, the probe motion is more restricted (compared to the situation without the dendrimers), and the probe concentrates in the CTAB aggregates adsorbed on the dendrimer surface.

C12T as a Probe of DTAB Micellization in the Absence and in the Presence of Dendrimers. Figure 3 shows some representative spectra of C12T (2×10^{-5} M) as a probe of DTAB solutions (2×10^{-3} M and 7×10^{-3} M) in the absence (a-i; b-i, respectively) and presence of 0.185 M 7.5 SBD (a-ii; b-ii, respectively). The spectrum of a solution of pure C12T (c) is also shown for comparison. The full lines are the experimental spectra and the dotted lines are the computed spectra from which the parameters reported in Table 1-Figure 3 were derived.

In the absence of dendrimers and DTAB, spectrum c was computed with the magnetic parameters m, and high exchange frequency (Table1-Figure 3), due to close radicals, which indicated the self-aggregation of the probes. This feature persisted by adding DTAB, even in the presence of relatively large concentrations of DTAB. For example, at [DTAB] = 7×10^{-3} M (spectrum b-i in Figure 3), about 50% of the C12T radicals still formed homomicelles and 50% formed mixed

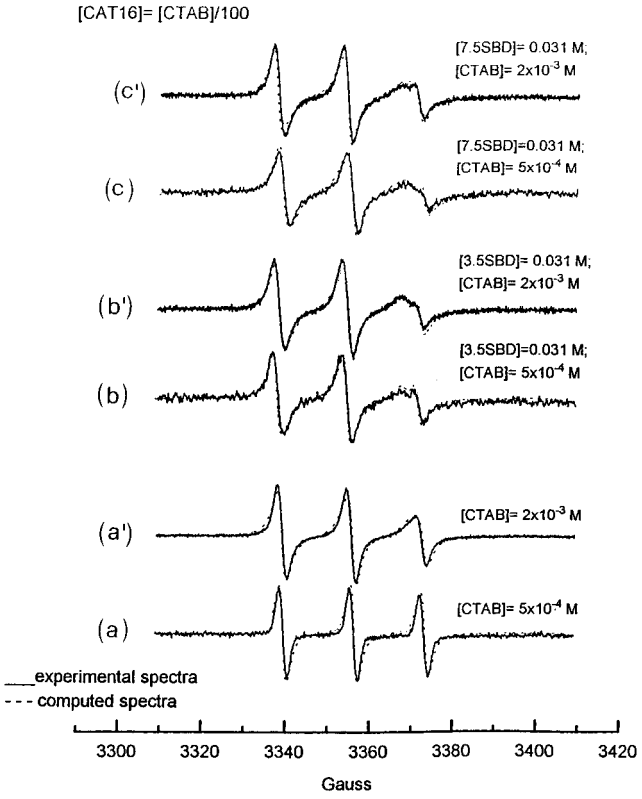

Figure 2. Experimental (full line, 303 K) and computed (dotted lines) EPR spectra of CTAB solutions (5×10^{-4} and 2×10^{-3} M) containing CAT16 at [CTAB]/[CAT16] = 100, in the absence and presence of 3.5 SBD and 7.5 SBD (0.031 M).

micelles with the DTAB surfactants. A progressive dilution of C12T radicals in DTAB micelles was observed above the DTAB cmc (results not shown).

In the presence of dendrimers, mixed micellar aggregates of C12T and DTAB were formed even in the presence of small amounts of DTAB, as evidenced by the disappearance of the spin−spin components in the probe spectrum as DTAB concentration was increased (spectra a-ii and b-ii in Figure 3).

CAT9 as a Probe of DTAB Micellization in the Absence and in the Presence of Dendrimers. Figure 4 shows some representative spectra of CAT9 as a probe of DTAB solutions in the absence and in the presence of dendrimers. The full lines are the experimental spectra and the dotted lines are the computed spectra from which the parameters reported in Table 1-Figure 4 were derived. Nearly identical line shapes were observed for 4×10^{-4} M solutions of DTAB containing CAT9 at 2×10^{-6} M in the absence of dendrimers (Figure 4a, dashed line (a)) and in the presence of 0.031 M 3.5 SBD or 0.185 M 7.5 SBD (Figure 4a, (b)). The spectral parameters are indicative of radicals, which are free in solution in the absence of dendrimers and gave primary noncooperative interactions with the dendrimer surface in the presence of dendrimers. The line shape changes for 0.185 M 3.5 SBD or 0.031 M 7.5 SBD, but the spectra were equivalent to each other in these two cases (Figure 4a, (c)). The parameters indicated that at least 65% of the probe molecules are inserted into DTAB aggregates at the dendrimer surface, with consequent decrease in mobility and environmental polarity of the probe (parameters in Table 1-Figure 4).

It is noteworthy that a higher concentration of 3.5 SBD and a lower concentration of 7.5 SBD were needed to promote the secondary cooperative interactions of DTAB with the dendrimer surface, even at DTAB concentrations well below the cmc. The formation of supramolecular structures composed of surfactant aggregates adsorbed on the dendrimer surface is inhibited for later generation dendrimer at high concentration. Evidently, the dimension of the supramolecular structure DTAB aggregate + 7.5 SBD was too large to form when several macromolecules were in solution.

In the absence of dendrimers, an increase of CTAB concentration causes CAT9 to insert into the DTAB micelles (results not shown). In the presence of dendrimers, DTAB aggregates are formed at the SBD surface in all generations and dendrimer concentrations investigated, but their formation is favored by low concentration of later generation dendrimers. These conclusions can be derived from Figure 4b (see also parameters in Table 1-Figure 4) for DTAB (1×10^{-3} M) and 3.5 SBD ((d) [CAT9] = 5×10^{-6} M; (e) [CAT9] = 5×10^{-5} M) and 7.5 SBD ([CAT9] = 5×10^{-5} M; (f) 303 K; (g) 333 K) (both the dendrimers at 0.185 M). An increase in [DTAB] from 4×10^{-4} to 1×10^{-3} M, for 3.5 SBD with [CAT9] = 5×10^{-6} M, led to a small variation of the fraction of radicals involved in aggregates (from 65% to 75%), whereas the other parameters remained constant. A constant ratio [DTAB/[CAT9] was maintained to ensure a negligible perturbation effect by the probe so that the structure of the aggregates did not change with the increase in DTAB concentration.

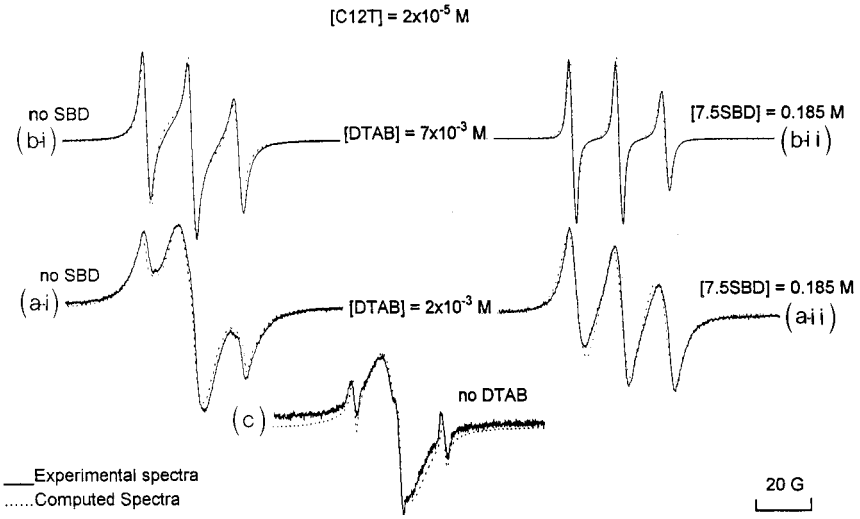

Figure 3. EPR experimental (full lines, 303 K) and computed (dotted lines) EPR spetcra of C12T (2×10^{-5} M) pure solution and as a probe of DTAB solutions (2×10^{-3} and 7×10^{-3} M), in the absence and in the presence of 0.185 M 7.5 SBD.

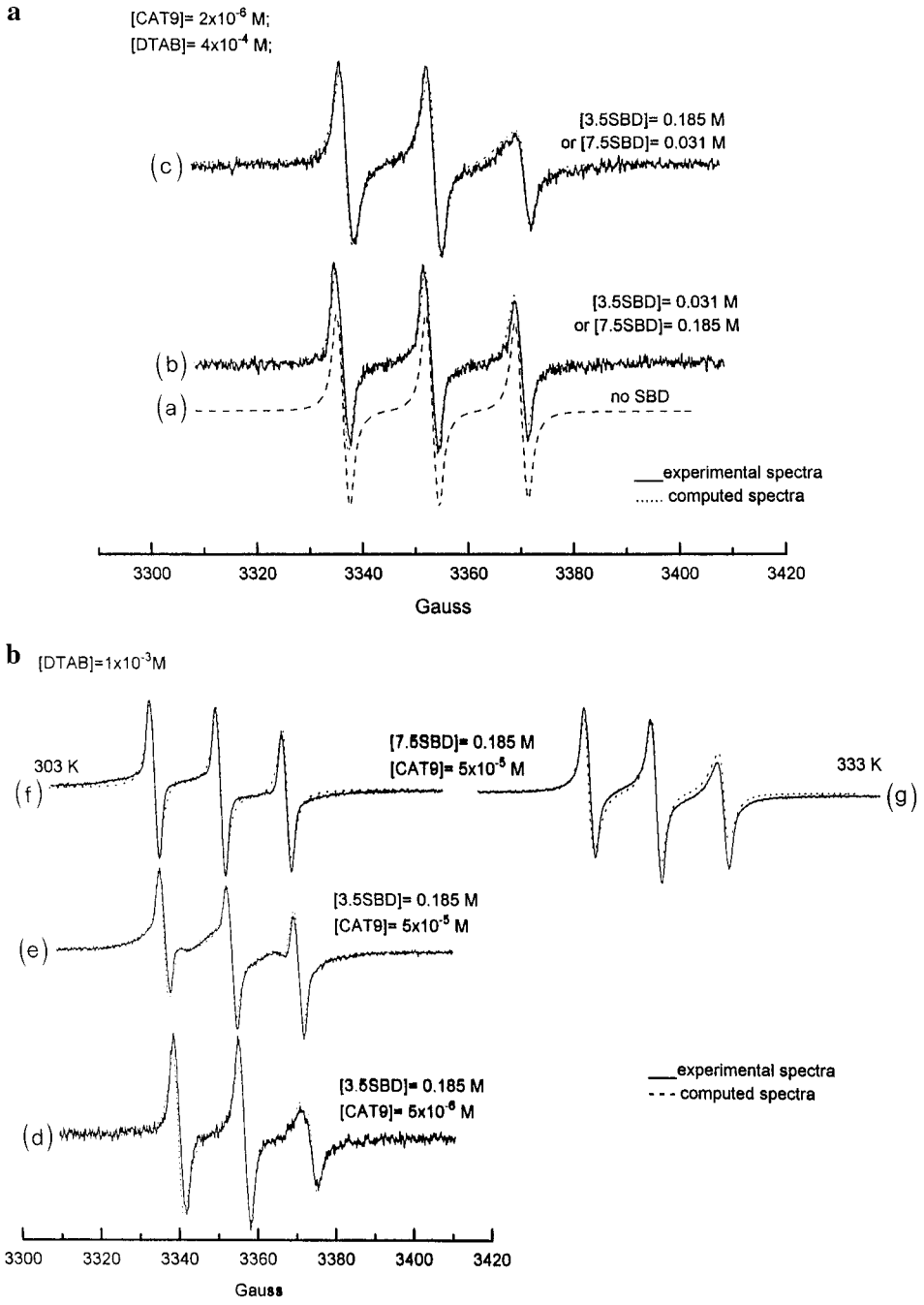

Figure 4. (a) Experimental (full lines, 303 K) and computed (dotted lines) EPR spectra of 4×10^{-4} M solutions of DTAB containing CAT9 at 2×10^{-6} M in the presence of 0.031 M 3.5 SBD or 0.185 M 7.5 SBD and in the presence of 0.031 M 7.5 SBD or 0.185 M 3.5 SBD. The dashed line in the bottom is the experimental spectrum of the DTAB + CAT9 solution in the absence of dendrimers. (b) Experimental (full lines) and computed (dotted lines) EPR spectra of DTAB solutions (1×10^{-3} M) in the presence of 3.5 SBD (0.185 M) and CAT9 at two concentrations (5×10^{-6} and 5×10^{-5} M) and in the presence of 7.5 SBD (0.185 M) and CAT9 (5×10^{-6} M) at two temperatures (303 and 333 K).

By increasing [CAT9] from 5×10^{-6} to 5×10^{-5} M for 3.5 SBD (Figure 4b, from (d) to (e)), most of the CAT9 radicals (95%) were adsorbed in DTAB aggregates. This effect is contrary to that observed for CAT16 and CTAB aggregates (*vide supra*), where a saturation adsorption of probe in the aggregates was invoked to explain the data. Thus, CAT9 is more effective in being adsorbed in the DTAB surfactant aggregates formed on the dendrimer surface than is the case for CAT16 in CTAB aggregates on the dendrimer surface. It was also found that mixed DTAB/CAT9 aggregates on the dendrimer surface containing more than one radical per aggregate were formed at high CAT9 concentration.

The small fraction of monomers (5%) remaining in solution in the presence of 0.185 M 3.5 SBD (spectrum (e) in Figure 4b) showed high mobility ($=5 \times 10^{-11}$ s), as found for free radicals in solution, not interacting with the dendrimer surface. Therefore, these free probes were prevented from binding the dendrimers with primary interactions. It is plausible that the positively charged aggregates at the surface neutralized the negative changes of the dendrimer surface, thereby neutralizing the electrostatic interaction with CAT9 monomers.

The sample of 7.5 SBD (0.185 M) with $[CAT9] = 5 \times 10^{-5}$ M again showed a lower relative fraction of the radicals involved in the aggregates (Figure 4b, (f)) with respect to 3.5 SBD at the same concentration (Figure 4b, (e)). The supramolecular dendrimer−aggregate structure in the presence of 7.5 SBD was too large to be formed in concentrated solutions, and primary interactions of the surfactant monomers with the dendrimer surface are to some extent preferred. However, more than one radical was hosted in each DTAB aggregate. An increase in

temperature was expected to increase the spin exchange frequency. But a different mechanism predominated with increasing temperature: high temperatures strongly promoted the insertion and distribution of probe molecules among the DTAB aggregates. At higher temperatures (Figure 4b, (g)) the system was more fluid and the radical mobility toward the aggregates was enhanced.

Conclusions: A Model To Describe the Negatively Charged Dendrimer−Positively Charge Surfactant System. Optimization of the EPR Spin Probe Method

The use of different surfactant spin probes and computer simulation of probes in EPR spectra to determine their mobility, the environmental polarity, and the partition in the various supramolecular structures produced by anionic dendrimer−cationic surfactant systems allows a detailed overview of these structures, since each probe monitors a different region or property of the system. Thus, the surfactant spin probe method may be improved by comparing results from probes differing from each other in properties such as the following: (1) position of the probe in the molecular structure with respect to other hydrophobic and hydrophilic portions of the surfactant chain; (2) the charge and polarity of the probe; (3) the self-aggregation ability of the probe; (4) the solubility of the probe in polar and nonpolar environments; and (5) the experimental conditions of concentration and temperature.

The main results obtained by this optimized probe method are summarized as follows.

(1) Aggregation of the surfactants in the presence of the dendrimers takes place at lower concentration than the cmc of the surfactant in aqueous solution; that is, the critical surfactant aggregation concentration, cac, < cmc.

(2) The low cac does not depend on the increase in ionic strength occurring upon addition of dendrimers, but depends on the dendrimer size and concentration; that is, the aggregation is favored in the presence of later generation dendrimers at low concentration.

(3) Supramolecular structures composed of surfactant aggregates adsorbed at the dendrimer water interface are formed. For later generation dendrimers at high concentration, the large size of the supramolecular structures is sterically inhibited and only a small number of surfactant aggregates can be formed in the solution existing between the dendrimer molecules.

(4) The surfactant aggregates may contain one or more probes, depending on the probe concentration. The solubility of the probes in the surfactant aggregates is enchanced by the presence of dendrimers. The positively charged probe CAT16 reaches a saturation condition in surfactant aggregates at the dendrimer surface. The solubility of the probes in the aggregates and the distribution and exchange among surfactant aggregates are enhanced by increasing temperature.

(5) Primary interactions of the probe with the dendrimer surface and secondary interactions of the probe belonging to surfactant aggregates formed on the dendrimer surface compete with one another, and the ratio of primary binding to secondary binding depends on the size of the supramolecular structures: large dendrimers (later generations) should form too large supramolecular structures with the surfactant aggregates, and their formation becomes unfavorable. Therefore, a large fraction of the surfactant and the probes give rise to primary, noncooperative interaction with the hydrophilic and hydrophobic sites of the later generation dendrimers.

Figure 5 shows a schematic model of the structures formed by cationic surfactants and anionic dendrimers. The model displays the following features.

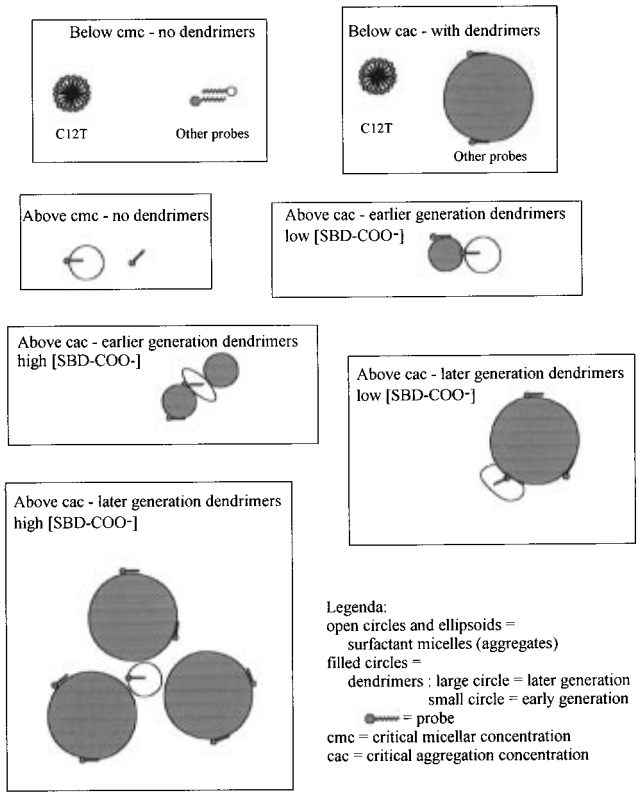

Figure 5. Schematic model for the interactions between anionic dendrimers and cationic surfactants.

(1) Below cmc, No Dendrimers. The EPR spectra were characteristic of probes free in solution, with the exception of C12T; in this case the spin−spin interactions indicated that C12T micelles were formed in the range of concentration of the probe detectability by EPR.

(2) Below cac, with Dendrimers. The rotational mobility of the probes decreased because of primary noncooperative interactions with the dendrimer surface, as already found for surfactant probes below cmc. The EPR spectra of C12T were unchanged; that is, C12T formed noninteracting micellar aggregates.

(3) Above cmc, No Dendrimers. The change from the "f" to the "m" set of magnetic parameters and the decrease in $\tau_{\perp}$ were consistent with the insertion of the probe in the surfactant micelles in correspondence with the cmc (with the exception of C12T, which only inserted in CTAB micelles at very high surfactant concentration). A fraction of the probes showed the same EPR line shape as the free radicals below the cmc. Therefore, surfactant micelles were formed that contained one or more probes in equilibrium with monomers in solution.

(4) Above cac, Earlier Generation Dendrimers, Low [SBD−COO⁻]. The mobility and the environmental polarity were modified with respect to those found for the probes in micelles in the absence of the dendrimers. Therefore, a different type of aggregate was formed at concentrations well below the cmc. We suggest that supramolecular structures originated from the surfactant aggregates and the dendrimers. The shape and size of the micelles were probably unmodified by the interaction with the dendrimers. The positively charged probes were mainly hosted in the aggregates at the dendrimer/aggregate interface. Secondary cooperative interactions were preferred to primary interactions.

(5) Above cac, Earlier Generation Dendrimers, High [SBD−COO⁻]. Further modification of the EPR parameters occurred at high SBD−COO⁻ concentrations and the formation

of surfactant aggregates at the dendrimer surface was favored even at very low concentrations of the surfactants. The suggested structure[9,10] is constituted by elongated micelles interacting with more than one dendrimer molecule. The high ionic strength, together with steric constraint due to the "sandwich" insertion among the dendrimers, supports the hypothesis of elongated (or oblate) micelles.

(6) Above cac, Later Generation Dendrimers, Low [SBD−COO⁻]. The magnetic and mobility parameters of the probe-surfactant systems in the presence of low [7.5 SBD] were comparable to those found in the presence of high [3.5 SBD]. Therefore, similar aggregate structures were suggested in the two cases, that is, oblate micelles interacting with the dendrimer surface. These supramolecular structures were highly favored at very low concentrations of the surfactants. The local high ionic strength and the steric adaptation to the dendrimer surface support the hypothesis of elongated (or oblate) micelles.

(7) Above cac, Later Generation Dendrimers, High [SBD−COO⁻]. With the increase in 7.5 SBD concentration, the EPR parameters of an increasing fraction of probes become similar to those found in the absence of the dendrimers. A fraction of surfactants, therefore, formed spherical micelles poorly interacting with the dendrimer surface. The large sized supramolecular structure was hardly accommodated in the viscous dendrimer solution. Primary noncooperative interactions become favored with respect to the secondary interactions.

Acknowledgment. N.J.T. thanks the NSF and NATO for their generous support. D.A.T. thanks the New Energy and Development Organization (NEDO) of the Ministry of International Trade and Industry of Japan (MITI) for the generous support and certain critical synthetic efforts. M.F.O. and P.A. thank the Italian Ministero Università e Ricerca Scientifica e Tecnologica (MURST), and the Italian Consiglio Nazionale delle Ricerche (CNR) for the financial support.

References and Notes

(1) (a) *Spin Labeling. Theory and Applications*; Berliner, L. J., Ed.; Academic Press: New York, 1976; Vol.1; 1979; Vol. 2. (b) *Biological Magnetic Resonance. Spin Labeling. Theory and Applications*; Berliner, L. J., Reuben, J., Eds.; Plenum Press: New York, 1989; Vol. 8.

(2) Taupin, C.; Dvolaitoky, M. In *Surfactant Solutions. New Methods of Investigation*; Zana, R., Ed.; Surfactant Science Series, Vol. 22; Marcel Dekker: New York, 1987; p 359.

(3) Hearing, G.; Luisi, P. L.; Hauser, H. *J. Phys. Chem.* **1983**, *92*, 3574.

(4) Yoshioka, H.; Kazama, S. *J. Colloid Interface Sci.* **1983**, *95*, 240.

(5) Wikander, G.; Johansson, L. B.-A. *Langmuir* **1989**, *5*, 728.

(6) (a) Baglioni, P.; Ferroni, E.; Martini, G.; Ottaviani, M. F. *J. Phys. Chem.* **1984**, *88*, 5187. (b) Baglioni, P.; Ottaviani, M. F.; Martini, G. *J. Phys. Chem*. **1986**, *90*, 5878.

(7) (a) Bales, B. L.; Kevan, L. *J. Phys. Chem.* **1982**, *86*, 3836. (b) Bratt, J. P.; Kevan, L. *J. Phys. Chem.* **1992**, *96*, 6849; **1993**, *96*, 6849.

(8) (a) Schreier, S.; Ernandes, J. R.; Cuccovia, I.; Chaimovich, H *J. Magn. Reson.* **1978**, *30*, 283, and references therein. (b) Ernandes, J. R.; Schreier, S.; Chaimovich, H. *Chem. Phys. Lipids* **1976**, *16*, 19. (c) Ernandes, J. R.; Chaimovich, H.; Schreier, S. *Chem. Phys. Lipids* **1977**, *18*, 304.

(9) Ottaviani, M. F.; Turro, N. J.; Jockusch, S.; Tomalia, D. A. *J. Phys. Chem.* **1996**, *100*, 13675.

(10) Ottaviani, M. F.; Turro, N. J.; Jockusch, S.; Tomalia, D. A. *Colloids Surf.* **1996**, *115*, 9.

(11) Goddard, E. D. *Colloids Surf.* **1986**, *19*, 255; **1986**, *19*, 301.

(12) Robb, I. D. In *Anionic Surfactants: Physical Chemistry of Surfactant Actions*; Lucassen-Reynders, E. H., Ed.; Marcel Dekker: New York, 1981; p 109.

(13) Goddard, E. D.; Hannan, K. B. In *Micellization, Solubilization and Microemulsions*; Mittal, K. L., Ed.; Plenum Press: New York, 1977; Vol. 2.

(14) Brackman, J. C.; Engberts, J. B. F. N. *Chem. Soc. Rev.* **1993**, 85.

(15) Gao, Z.; Kwak, J. C. T.; Labonte, R.; Marangoni, G.; Wasylishen, R. E. *Colloids Surf.* **1990**, *45*, 269.

(16) *Advances in Dendritic Macromolecules*; Newkome, G. R., Ed.; JAI Press: Greenwich, CT, 1993.

(17) (a) Krohn, K. Starburst Dendrimers and Arborols. *Org. Synth. Highlights* **1991**, 378. (b) Amato, L., Trekking in the Molecular Forest. *Sci. News* **1990**, *138*, 298. (c) Newkome, G. R.; Moorefield, C. N.; Baker, G. R.; Johnson, A. L.; Behera, R. K. *Angew. Chem., Int. Ed. Engl.* **1991**, *30*, 1176. (d) Newkome, G. R.; Moorefield, C. N.; Baker, G. R.; Saunders, M. J.; Grossman, S. H. *Angew. Chem., Int. Ed. Engl.* **1991**, *30*, 1178. (e) Kim, Y. H.; Webster, O. W. *J. Am. Chem. Soc.* **1990**, *112*, 4592. (f) Hawker, C. J.; Wooley, K. L.; Fréchet, J. M. J. *J. Chem. Soc., Perkin Trans. 1* **1993**, 1287. (g) Newkome, G. R.; Young, J. K.; Baker, G. R.; Potter, R. L.; Audoly, L; Cooper, D.; Weis, C. D. *Macromolecules* **1993**, *26*, 2394.

(18) (a) Tomalia, D. A.; Baker, H.; Dewald, J.; Hall, M.; Kallos, G.; Martin, S.; Roeck, J.; Smith, P. *Polym. J. (Tokyo)* **1985**, *17*, 117. (b) Tomalia, D. A.; Hall, M.; Hedstrand, D. M. *J. Am. Chem. Soc.* **1987**, *109*, 1601. (c) Wilson, L. R.; Tomalia, D. A. *Polym. Prepr. (Am. Chem. Soc. Div. Polym. Chem.)* **1989**, *30*, 115. (d) Padias, A. B.; Hall, H. K.; Tomalia, D. A. *Polym. Prepr. (Am. Chem. Soc. Div. Polym. Chem.)* **1989**, *30*, 119. (e) Meltzer, A. D.; Tirell, D. A.; Jones, A. A.; Inglefield, P. T.; Downing, D. M.; Tomalia, D. A. *Polym. Prepr. (Am. Chem. Soc. Div. Polym. Chem.)* **1989**, *30*, 121. (f) Tomalia, D. A.; Naylor, A. M.; Goddard, W. A., III. *Angew Chem., Int. Ed. Engl.* **1990**, *29*, 138.

(19) Ottaviani, M. F.; Bossmann, S.; Turro, N. J.; Tomalia, D. A. *J. Am. Chem. Soc.* **1994**, *116*, 661.

(20) Ottaviani, M. F.; Montalti, F.; Turro, N. J.; Tomalia, D. A. *J. Phys. Chem*. **1996**, *100*, 11033.

(21) Naylor, A. M.; Goddard, W. A., III; Kiefer, G. E.; Tomalia, D. A. *J. Am. Chem. Soc.* **1989**, *111*, 2341.

(22) Ottaviani, M. F.; Cossu, E.; Turro, N. J.; Tomalia, D. A. *J. Am. Chem. Soc.* **1995**, *117*, 4387.

(23) Dvornic, P. R.; Tomalia, D. A. *Macromol. Symp.* **1994**, *88*, 123.

(24) Berr, S. S. *J. Phys. Chem.* **1987**, *91*, 4760.

(25) Caminati, G.; Turro, N. J.; Tomalia, D. A. *J. Am. Chem. Soc.* **1990**, *112*, 8515.

(26) Schneider, D. J.; Freed, J. H. in *Biological Magnetic Resonance. Spin Labeling. Theory and Applications*; Berliner, L. J., Reuben, J., Eds.; Plenum Press: New York, 1989; Vol. 8, p 1.

(27) (a) Janzen, E. G. *Top. Stereochem.* **1971**, *6*, 117. (b) Ottaviani, M. F.; Martini, G.; Nuti, L. *Magn. Reson. Chem.* **1987**, *25*, 897.

(28) (a) Plachy, W.; Kivelson, D. *J. Chem.Phys.* **1967**, *47*, 3312. (b) Sackmann, E.; Träuble, T *J. Am. Chem. Soc.* **1972**, *94*, 4482, 4492, 4499. (c) Aizawa, M.; Komatsu, T.; Nakagawa, T. *Bull. Chem. Soc. Jpn.* **1979**, *52*, 980; **1980**, *53*, 975.